

Lawrence Berkeley National Laboratory

LBL Publications

Title

Enhancement of Laser Injection Methods by Plasma Density Gradients

Permalink

<https://escholarship.org/uc/item/5mm4x8qs>

Authors

Fubiani, G.
Esarey, E.
Nakamura, K.
et al.

Publication Date

2004

Enhancement of Laser Injection Methods by Plasma Density Gradients

G. Fubiani^{*†}, E. Esarey^{*}, K. Nakamura^{*‡}, C. B. Schroeder^{*} and W. P. Leemans^{*}

^{*}*Lawrence Berkeley National Laboratory, University of California, Berkeley, CA 94720 USA*

[†]*University of Paris XI, Orsay, France*

[‡]*University of Tokyo, Japan*

Abstract. Plasma density down-ramps are proposed as a method for improving the performance of laser injection schemes. A decrease in density implies an increase in plasma wavelength, which can shift a relativistic electron from the defocusing to the focusing region of the accelerating wakefield. Also, a decrease in density leads to a decrease in wake phase velocity, which lowers the trapping threshold. The specific method of two-pulse colliding pulse injector was examined using a 3D test particle tracking code. A density down-ramp of 30% led to an order of magnitude enhancement of the trapping fraction compared to the uniform plasma case, without degrading other bunch properties.

INTRODUCTION

Compared to standard radio-frequency (RF) linear accelerators, plasma accelerators can produce acceleration gradients in excess of 10 GeV/m without the limitation of breakdown. In a plasma, the wavelength of the acceleration field is the plasma wavelength, $\lambda_p = 2\pi c/\omega_p$, where $\omega_p = (4\pi n_0 e^2/m_e)^{1/2}$ is the plasma frequency and n_0 is the plasma density. For example, a laser wakefield accelerator (LWFA) [1] in the standard regime typically has a density on the order of $n_0 \simeq 10^{18} \text{ cm}^{-3}$ and a plasma wavelength on the order of $\lambda_p \simeq 30 \text{ }\mu\text{m}$. If a mono-energetic electron bunch is injected into a wakefield such that it is accelerated while maintaining a small energy spread, then it is necessary for the bunch to occupy a small fraction of the wake period, on the order of a few fs, which requires fs accuracy in the injection process. These requirements are beyond the current state-of-the-art performance of photocathode RF electron guns.

Several methods for injecting plasma electrons into the wakefield have been proposed. One of them relies on self-injection using a single laser pulse in an inhomogeneous plasma [2], where trapping occurs from wave breaking induced on a downward density ramp. Another mechanism relies on ponderomotive acceleration using two lasers [3, 4], where one (injection) laser pulse intersects the plasma wake generated by the other (drive) laser pulse. Injection results from the ponderomotive force of the injection pulse on the electrons in the plasma wake. In the original colliding pulse injector (CPI) method, three short laser pulses were used for electron injection [5]. The pump pulse generates a plasma wake through its ponderomotive force, as in the standard laser wakefield accelerator (LWFA). The two injection pulses, one pulse propagating in the

forward and one in the backward direction, collide at a predetermined phase of the plasma wake behind the pump pulse. During this collision, the beating of the injection laser pulses generates a beat wave that shifts the phase and momentum of a subset of the background electrons, which then can be trapped and accelerated. Since the force associated with the laser beat wave is larger than the ponderomotive force from a single pulse, the CPI method is more efficient than ponderomotive injection with a single injection pulse.

A simplified configuration of the CPI concept was proposed and analyzed by Fubiani et al [6]. It uses only two laser pulses with parallel polarizations: an intense pump pulse for wakefield generation and a single counterpropagating (or propagating at a finite angle) injection pulse. Injection is the result of the laser beat wave produced when the backward injection pulse collides and interferes with the trailing portion of the pump pulse. This configuration has the advantages of being easier to implement in comparison to the three-pulse CPI scheme, and of requiring less intensity in the injection pulse compared to the ponderomotive injection scheme.

Here a negative plasma density gradient is proposed as a method for enhancing the electron beam quality in laser injection schemes. If a laser injection scheme is operated close to threshold, electrons will be injected into the region of the wake that is accelerating but defocusing. To have a trapped electron bunch that is both accelerated and focused, it is necessary to shift the bunch forward in phase. This can be accomplished with a downward density ramp. As the density decreases, the plasma wavelength increases, thus a relativistic electron will be shifted forward in phase relative to the wake. This can shift an electron from the defocusing to the focusing region of the accelerating wake. In addition, if injection occurs on the density down-ramp, the trapping can occur more readily since the phase velocity of the wake is lowered on the down ramp. Numerical examples are given based on a three dimensional (3D) particle tracking code for the specific case of the two-pulse CPI method with density gradients.

DENSITY DOWN-RAMPS

A density down-ramp can enhance the number of trapped and focused electrons by two effects: (1) A decrease in density shifts the position of an electron forward in phase with respect to the wakefield and (2) a decrease in density decreases the phase velocity of the wake, thus providing a lower threshold for injection. Consider a change in density from n_i to n_f ($n_i > n_f$) over a length L_t . The phase of the electron before and after the transition are given by $\psi_i = k_{pi}\zeta$ and $\psi_f = k_{pf}\zeta$, respectively, assuming that the slippage between the electron and the drive laser pulse is small over L_t (ζ is approximately constant), where $\zeta = z - ct$ is the position of the electron behind the drive pulse ($\zeta < 0$ behind the drive pulse), and $k_{pi} = \omega_{pi}/c$ and $k_{pf} = \omega_{pf}/c$ are the plasma wavenumbers evaluated at n_i and n_f , respectively. Hence, the change in phase of the electron after the density transition is $\Delta\psi = \psi_i - \psi_f$, i.e.,

$$\Delta\psi = \psi_i[1 - (n_f/n_i)]^{1/2} \simeq \psi_i(\Delta n/n_i)^{1/2}, \quad (1)$$

assuming $\Delta n = n_i - n_f \ll n_i$. Hence, the change in density required to shift and electron forward in phase by a small amount (e.g., $\Delta\psi \sim \pi/4$) is $\Delta n/n_i = (\Delta\psi/\psi_i)^2 = (\Delta\psi/k_p\zeta)^2$. Note that rephasing becomes easier (a smaller $\Delta n/n_i$ is required) with increasing distance behind the driver (larger $|\zeta|$). Hence, rephasing is more efficient for the three-pulse CPI configuration than for two-pulse CPI, assuming the injection point for three-pulse CPI is behind the first wake period.

If the injection (pulse collision) point was to occur on the down-ramp (as opposed to prior to it), then trapping could be further enhanced due to the decrease in phase velocity of the wake on the down-ramp. The wake phase velocity v_p can be calculated from the wake phase $\psi = k_p(z - ct)$ via $d\psi/dt = 0$. This gives

$$v_p/c = k_p/(k_p + \zeta dk_p/dz), \quad (2)$$

where $dk_p/dz = (k_p/2n)dn/dz$. Since $\zeta < 0$ behind the drive pulse, the phase velocity decreases on a density down-ramp ($dn/dz < 0$). Note that this effect becomes more pronounced the larger the distance behind the driver. Thus, the reduction in phase velocity due to the down-ramp is potentially more effective for three-pulse CPI than for two-pulse CPI. Eventually, even in the absence of an injection pulse, the down-ramp leads to wavebreaking and injection for a sufficiently large distance behind the pump pulse [2], assuming that the wake amplitude does not damp.

FIELDS OF LASER AND WAKE

This section describes the prescribed laser and wake fields (obtained from linear wake-field theory) used in the 3D particle tracking code. The laser fields of the pump ($i = 0$) and injection ($i = 1$) laser pulses are described by the normalized vector potentials $\mathbf{a}_i = e\mathbf{A}_i/m_e c^2$. Using the paraxial wave equation with a linear plasma response, the transverse laser fields (linearly polarized in the x -direction and propagating along the z -axis) are given by [7] $a_{xi}(r, \zeta_i) = \hat{a}_i(r, \zeta_i) \cos \psi_i$ with

$$\hat{a}_i(r, \zeta_i) = a_i(r_i/r_{si}) \exp(-r^2/r_{si}^2) \sin(\pi\zeta_i/L_i), \quad (3)$$

for $-L_i < \zeta_i < 0$ and zero otherwise, where $\zeta_0 = z - \beta_{g0}ct$ (forward comoving coordinate), $\zeta_1 = z + \beta_{g1}ct$ (backward comoving coordinate), $\beta_{gi} = \eta_i$ is the linear group velocity, $\beta_{\phi i} = \eta_i^{-1}$ is the linear phase velocity, $\eta_i = [1 - \omega_p^2/\omega_i^2 - 4/(k_i r_i)^2]^{1/2}$ is the plasma index of refraction, $\psi_i = k_i(z - \beta_{\phi i}ct) + \alpha_i r^2/r_{si}^2 + \alpha_i - \tan^{-1} \alpha_i$ is the phase, $k_i = \omega_i/(\beta_{\phi i}c)$ is the wavenumber, $\omega_i = 2\pi c/\lambda_i$ is the frequency in vacuum, $r_{si}(z) = r_i(1 + \alpha_i)^{1/2}$ is the spot size, r_i is the spot size at waist (here chosen to be $z = Z_{fi}$), $\alpha_i(z) = (z - Z_{fi})^2/Z_{Ri}^2$, $Z_{Ri} = k_i \eta_i r_i^2/2$ is the Rayleigh length, L_i is the pulse length, and a constant has been omitted in the definition of ψ_i that represents the initial position and phase of the laser pulse. Here, the pulse amplitude a_i is related to the intensity I_i by $a_i \simeq 8.6 \times 10^{-10} \lambda_i [\mu\text{m}] I_i^{1/2} [\text{W}/\text{cm}^2]$. The axial component of the laser field is specified via $\nabla \cdot \mathbf{a}_i = \mathbf{0}$. Keeping only the leading order contributions gives

$$a_{zi}(r, \zeta_i) \simeq 2x[\hat{a}_i(r, \zeta_i)/(k_i r_{si}^2)] (\sin \psi_i - \alpha_i \cos \psi_i). \quad (4)$$

Included in the simulations presented are the wakefields generated by both the pump and injection laser pulses. In the linear ($\langle a_i^2 \rangle \ll 1$) three-dimensional (3D) regime, wakefield generation can be examined using the cold fluid equations. For linear polarization and a slowly varying density variation ($L_t \gg \lambda_p$) the normalized electric field of the wakefield \mathbf{E}_i/E_0 is given by

$$[\partial^2/\partial\zeta_i^2 + k_p^2(z)] \mathbf{E}_i/E_0 \simeq k_p^2(z)\nabla\hat{a}_i^2/4, \quad (5)$$

where $E_0 = m_e c^2 k_{p0}/e$ is the cold nonrelativistic wavebreaking field normalized to a fixed ion density n_{00} . Note that a time-averaging has been performed over the fast laser oscillation (laser frequency), i.e., $\langle \hat{a}_i^2 \cos^2 \psi_i \rangle = \hat{a}_i^2/2$. Using the independent variables $\zeta = z - ct$ and z , and assuming that \hat{a}_i is a function of ζ_i only, the solution to Eq. (5) is

$$\mathbf{E}_i(r, \zeta_i)/E_0 = -(k_p(z)/4) \int_0^{\zeta_i} d\zeta'_i \sin[k_p(z)(\zeta_i - \zeta'_i)] (\partial/\partial\zeta'_i + \nabla_\perp) \hat{a}_i^2(r, \zeta'_i). \quad (6)$$

For the pulse profile given by Eq. (3), the electric field generated inside the pulse ($-L_i < \zeta_i < 0$) is

$$\frac{E_{ri}}{E_0} = \frac{a_i^2 r_i^2 r}{2 r_{si}^4} e^{-2r^2/r_{si}^2} \left[1 + \frac{(4\pi^2/k_p^2 L_i^2) \cos(k_p \zeta_i) - \cos(2\pi\zeta_i/L_i)}{(1 - 4\pi^2/k_p^2 L_i^2)} \right], \quad (7)$$

$$\frac{E_{zi}}{E_0} = k_p \frac{a_i^2 r_i^2}{8 r_{si}^2} e^{-2r^2/r_{si}^2} \left[\frac{(4\pi^2/k_p^2 L_i^2) \sin(k_p \zeta_i) - \sin(2\pi\zeta_i/L_i)}{(1 - 4\pi^2/k_p^2 L_i^2)} \right], \quad (8)$$

and behind the pulse ($\zeta_i < -L_i$),

$$\frac{E_{ri}}{E_0} = a_i^2 \frac{r_i^2 r}{r_{si}^4} e^{-2r^2/r_{si}^2} \left(\frac{4\pi^2}{k_p^2 L_i^2} \right) \frac{\sin[k_p(\zeta_i + L_i/2)] \sin(k_p L_i/2)}{(1 - 4\pi^2/k_p^2 L_i^2)}, \quad (9)$$

$$\frac{E_{zi}}{E_0} = -k_p \frac{a_i^2 r_i^2}{4 r_{si}^2} e^{-2r^2/r_{si}^2} \left(\frac{4\pi^2}{k_p^2 L_i^2} \right) \frac{\cos[k_p(\zeta_i + L_i/2)] \sin(k_p L_i/2)}{(1 - 4\pi^2/k_p^2 L_i^2)}. \quad (10)$$

The initial plasma density profile is assumed to be of the form $n_0(z)/n_{00} = 1 - (\tau_t/2)[1 + \tanh(z/L_t)]$, where n_{00} is the density before the density transition ($z < 0$) and $\tau_t = \Delta n_0/n_{00}$ the relative change of density.

Note that for high laser intensities ($|a_i| > 1$), this model becomes inaccurate. To describe the nonlinear regime in 3D, as well as other nonlinear effects such as beam loading, requires self-consistent simulations such as can be done with particle-in-cell codes, which is beyond the scope of this paper. In the following simulations, the plasma was modeled by a group of test electrons initially at rest and loaded randomly in a 3D spatial region of length λ_p and transverse size $\lambda_p \times \lambda_p$, uniformly about the z -axis. This spatial region was chosen to be ahead of the pump laser pulse, and timed with respect to the initial position of the injection pulse such that when the two pulses collide, the test electrons fill the entire region in which trapping may occur. After the collision, various

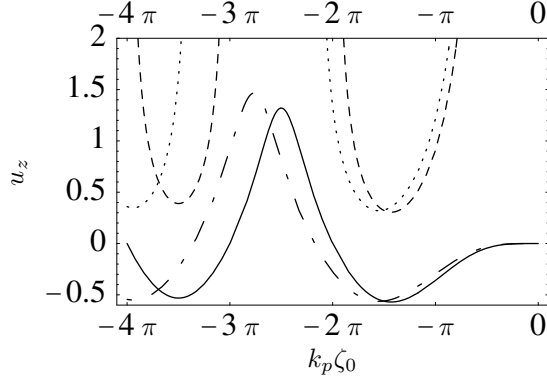


FIGURE 1. Phase space plot showing cold fluid orbit for $n_0/n_{00} = 1$ (solid line) $n_0/n_{00} = 0.7$ (dot-dashed line), trapped and focused orbit for $n_0/n_{00} = 1$ (dashed line), $n_0/n_{00} = 0.7$ (dotted line), with laser parameters: $L_0 = \lambda_p$ and $a_0 = 1.3$.

properties of the trapped electron bunch were monitored as a function of propagation time, such as the mean energy, the energy spread, the root-mean square (RMS) bunch length, and the trapping fraction. Here, the trapping fraction is defined as N_b/N_s where N_b is the number of electrons in the bunch and N_s the total number of test electrons.

SIMULATION RESULTS

In the simulations, the center of the density down ramp was set to coincide with the collision point of the injection and pump laser pulses. A quasi-1D configuration with $r_i \simeq \lambda_p$ was chosen, such that most of the injected electrons, although in a defocusing region of the accelerating wave, will only slowly depart transversely from their initial on-axis location. A density down-ramp will then rephase those electrons onto a trapped and focused orbit. This is shown in Fig. 1, where the cold fluid orbit and trapped and focused orbit are both shown for an initial density n_{00} and another density 30% smaller. Note that the focusing region has been extended farther behind the pump pulse.

The simulations were carried out for normalized laser-plasma parameters $a_0 = 1$, $\omega_0/\omega_{p0} = 50$, $L_0 = 9\lambda_{p0}/8$, $\omega_1/\omega_{p0} = 50$, $L_1 = \lambda_{p0}/2$, $k_{p0}L_t = 2\pi$ and $\tau_t = 30\%$. Figure 2 shows the resulting electron beam parameters produced in a uniform plasma [Fig. 2(a)] and using a 30% density down-ramp [Fig. 2(b)]. This shows a charge per bunch enhancement by a factor of ~ 12 for the case where $\lambda_0 = 0.8 \mu\text{m}$ and $n_{00} = 6.9 \times 10^{19} \text{ cm}^{-3}$ (i.e., $\lambda_{p0} = 40 \mu\text{m}$) was assumed.

For high bunch charge, beam-loading effects become important. This has been evaluated in Fig. 2, where $\delta n/n_0$ and E/E_0 are, respectively, the density variation and normalized electric field in the plasma from charge density n_b/n_0 of the electron bunch alone. For a uniform beam profile $n_b(r, \zeta) = n_b \Theta(r_b - r) \Theta(-\zeta) \Theta(\zeta + \sigma_z)$ of radius r_b and length σ_z , where Θ is a step function, the amplitude of the perturbed density and the

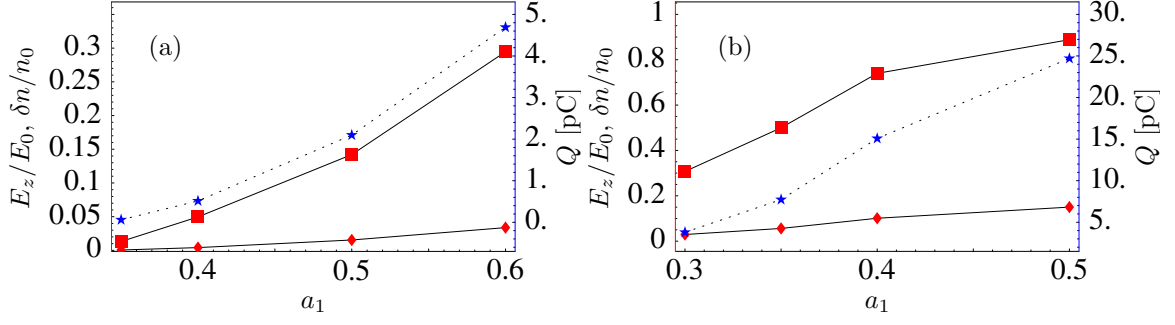


FIGURE 2. (Color) Bunch charge Q in pC (right vertical axis, stars), normalized axial electric field E_z/E_0 (left vertical axis, points), and normalized density perturbation $\delta n/n_0$ (left vertical axis, squares) generated by the electron bunch alone versus a_1 for (a) uniform plasma and (b) using a 30% density down-ramp. Laser-plasma parameters: $\lambda_0 = 0.8 \mu\text{m}$, $\lambda_{p0} = L_0 = r_0 = 40 \mu\text{m}$, $a_0 = 1$, $z_t = 0$, $L_t = \lambda_{p0}$, $\tau_t = 30\%$ and $ct = 47 k_{p0}^{-1} \simeq 300 \mu\text{m}$ after injection point.

axial electric field of the bunch-induced wake are given by [6, 8, 9]

$$\delta n/n_0 \simeq k_p \sigma_z n_b / n_0, \quad (11)$$

$$E_z/E_0 \simeq k_p \sigma_z F_R(r) n_b / n_0, \quad (12)$$

assuming $k_p \sigma_z \ll 1$, $\delta n/n_0 \ll 1$, and $E_z/E_0 \ll 1$, where the radial profile function is $F_R(r) = 1 - k_p r_b K_1(k_p r_b) I_0(k_p r)$ for $r < r_b$. Here I_0 and K_1 are modified Bessel functions. For a narrow beam $k_p^2 r_b^2 \ll 1$ and along the axis $F_R(r=0) \simeq [0.308 - 0.5 \ln(k_p r_b)] k_p^2 r_b^2$.

Figure 3 shows the electron beam properties as a function of injection laser strength a_1 for the same parameters as Fig. 2. As a_1 increases, trapping becomes more efficient, with corresponding increases in f_{tr} , $\Delta\gamma/\gamma$, σ_z/λ_{p0} , and r_b/λ_{p0} . The bunch emittance is approximated as $\epsilon_{\perp} = \gamma_0 \beta_0 (\langle x^2 \rangle \langle x'^2 \rangle)^{1/2} \simeq (\langle x^2 \rangle \langle u_x^2 \rangle)^{1/2}$, where $u_0 = \gamma_0 \beta_0 \simeq \gamma_0$ is the axial momentum of the electron bunch. The energy spread $\Delta\gamma/\gamma$ is on the order

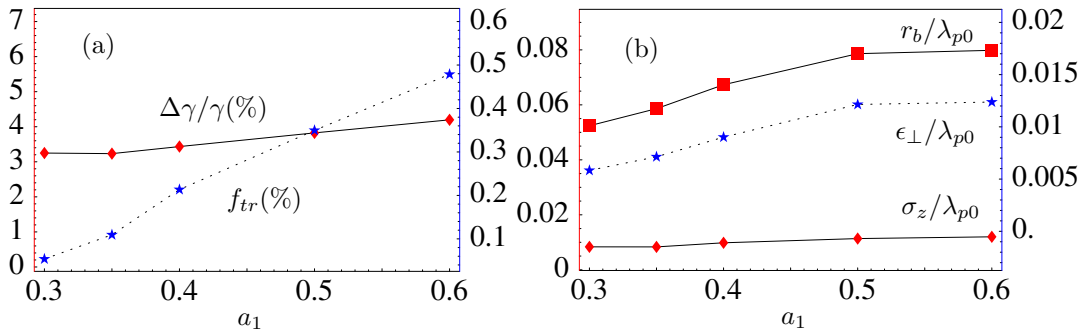


FIGURE 3. (Color) Trapped bunch parameters versus a_1 for $a_0 = 1$, $\omega_0/\omega_{p0} = 50$, $L_0 = 9\lambda_{p0}/8$, $\omega_1/\omega_{p0} = 50$, $L_1 = \lambda_{p0}/2$, $k_{p0} L_t = 2\pi$, $\tau_t = 30\%$ and $ct = 47 k_{p0}^{-1}$ after injection point. (a) Trapping fraction f_{tr} (right vertical axis) and relative energy spread $\Delta\gamma/\gamma$ (left vertical axis). (b) Bunch length σ_z/λ_{p0} (left vertical axis), RMS radius r_b/λ_{p0} (left vertical axis), and normalized transverse RMS emittance $\epsilon_{\perp}/\lambda_{p0}$ (right vertical axis).

of a percent, and the geometric emittance is $\tilde{\epsilon}_{\perp} \simeq (\langle x^2 \rangle \langle x'^2 \rangle)^{1/2} = 0.03$ mm-mrad for $\lambda_{p0} = 40 \mu\text{m}$. The bunch energy is approximately 6.5 MeV at $ct = 47 k_{p0}^{-1} \simeq 300 \mu\text{m}$ after the injection point. This will increase for longer acceleration lengths. It has also been found that varying L_t over a range $L_t = \lambda_{p0} - 3\lambda_{p0}$ does not change the electron beam parameters. This suggests the possibility of using density transition lengths $\sim 100 \mu\text{m}$, which is experimentally feasible with gas jets.

CONCLUSION

Plasma density down-ramps have been proposed as a method for improving electron bunch quality in laser injection schemes. A decrease in density implies an increase in plasma wavelength, which can shift a relativistic electron from the defocusing to the focusing region of the accelerating wakefield. Also, a decrease in density leads to a decrease in wake phase velocity, which can lower the trapping threshold. The specific method of two-pulse CPI was examined using a 3D test particle tracking code. A density down-ramp of 30% led to an order of magnitude enhancement of trapping fraction of background plasma electrons. Furthermore, no degradation of overall bunch parameters was observed compared to the uniform plasma case, even though the charge was an order of magnitude greater.

ACKNOWLEDGMENTS

This work was supported by the U.S. Department of Energy, Contract No. DE-AC-03-76SF0098.

REFERENCES

1. For a review see, E. Esarey et al., IEEE Trans. Plasma Sci. **PS-24**, 252 (1996).
2. S. Bulanov et al., Phys. Rev. E **58**, 5257 (1998).
3. D. Umstadter et al., Phys. Rev. Lett. **76**, 2073 (1996).
4. R.G. Hemker et al., Phys. Rev. E. **57**, 5920 (1998).
5. E. Esarey et al., Phys. Rev. Lett. **79**, 2682 (1997); C.B. Schroeder et al., Phys. Rev. E **59**, 6037 (1999).
6. G. Fubiani et al., Phys. Rev. E **70**, 016402 (2004).
7. E. Esarey and W. P. Leemans, Phys. Rev. E **59**, 1082 (1999).
8. R. Keinigs and M.E. Jones, Phys. Fluid **30**, 252 (1987).
9. T. Katsouleas et al., Part. Accel. **22**, 81 (1987).